

Bootstrap Current in TFTR

M. C. Zarnstorff, M. G. Bell, M. Bitter, R. J. Goldston, B. Grek, R. J. Hawryluk, K. Hill, D. Johnson, D. McCune, H. Park, A. Ramsey, G. Taylor, and R. Wieland

Plasma Physics Laboratory, Princeton University, Princeton, New Jersey 08544

(Received 28 December 1987)

Neutral-beam-heated plasmas in TFTR show evidence of substantial non-Ohmically driven toroidal current, even for balanced beam momentum input. The observations are inconsistent with calculations including only Ohmic and beam-driven currents, and presently can only be matched by models including the neoclassical bootstrap current.

PACS numbers: 52.25.Fi, 52.30.Bt, 52.50.Gj, 52.55.Fa

The electric current parallel to the magnetic field in a tokamak plasma is typically generated by an inductive electric field (Ohmic current). Many other mechanisms have been found or proposed for driving current,¹ including injection of fast particles² and perpendicular gradients of density and temperature.^{3,4} In the first case, the injected nonthermal particles directly carry the current, and are partially shielded by the collisional response of the thermal electrons. Such currents, carried by fast ions from injected neutral beams, have been previously studied in axisymmetric toroidal devices^{5,6} and stellarators⁷ and found to be in reasonable agreement with theory. In the latter case, neoclassical theory predicts nonzero off-diagonal coefficients in the Onsager transport matrix coupling the perpendicular (to the magnetic field) gradients of plasma density and temperature to the parallel electric current (the "bootstrap" current). This current has the potential for generation of a steady-state tokamak,^{4,8} and for driving MHD instabilities. Previous attempts to compare measured currents with the predicted bootstrap current in stellarators^{7,9-11} and an initial attempt in a tokamak¹² were unsuccessful or inconclusive. However, studies in a toroidal multipole¹³ showed good agreement with theory. Studies in stellarators have been hampered, until recently,¹⁴ by the lack of adequate theoretical treatment. Studies in tokamaks are complicated by the strong Ohmic current, long resistive equilibration times, and the difficulty of measurement of the local current density.

The Tokamak Fusion Test Reactor (TFTR) is heated by four tangential neutral-beam lines providing as much as 20 MW of D^0 at ≈ 100 keV for up to 2 sec. Three of the beam lines inject neutrals parallel (coinjection) to the toroidal plasma current I_p , and one injects antiparallel (counterinjection), allowing the input angular momentum to be varied by choice of operating beams. Feedback loops control I_p and the location of the outermost flux surface. The deuterium plasmas discussed here are of the enhanced confinement type obtained recently,¹⁵ and have $I_p = 0.8$ – 1.1 MA, toroidal magnetic field $B_T = 4.8$ – 5.2 T, major radius $R = 2.5$ m, and minor radius $a = 0.8$ m. With neutral-beam power P_B from 10

to 15 MW, and relatively low net injected momentum (nearly balanced coinjection and counterinjection), they typically have central electron temperature $T_e(0) \approx 8$ keV, central ion temperature $T_i(0) = 15$ – 30 keV, effective charge $Z_{\text{eff}} = 2$ – 4 , low toroidal rotation velocity $v_\phi \approx 10^5$ m/sec, and very peaked density profiles $n_e(0)/\bar{n}_e \approx 2.5$. These plasmas are in the collisionless regime with $v_{*i} < 5 \times 10^{-3}$, $v_{*e} < 5 \times 10^{-2}$ at $r = 0.3$ m, and have very long resistive equilibration times (≈ 5 sec). The typical time evolution of global parameters is shown in Fig. 1. The measured diamagnetic $\beta_{P\perp} \approx 2$, $\Lambda = \beta_{P\text{eq}} + I_i/2 \approx 3$, and Shafranov shift ≈ 0.35 m (from Thomson scattering density and temperature profiles). The elongation of the outermost flux surface (as inferred

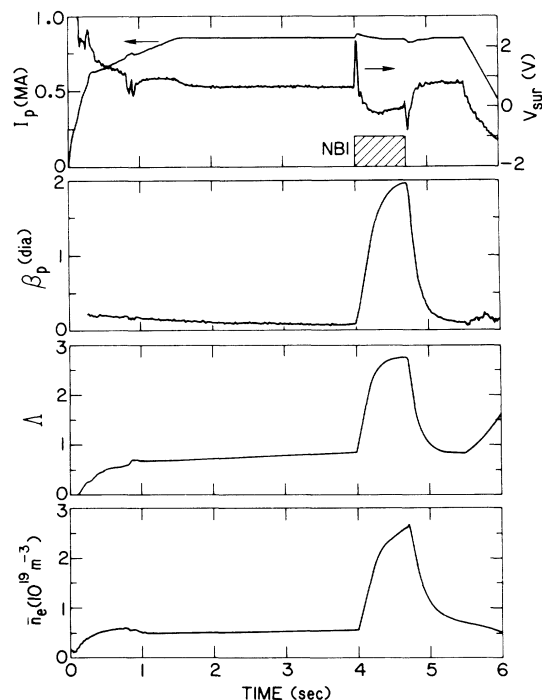


FIG. 1. Typical time dependence of plasma parameters I_p , $\beta_{P\perp}$, Λ , and \bar{n}_e . This plasma was heated by 10.6 MW of neutral beams from 4.0 to 4.7 sec, with $P_{\text{co}}/P_B = 0.57$.

from measurements of the poloidal field outside the plasma) decreases from 1.05 in the Ohmic phase to ≈ 0.9 at the end of beam heating. Unidirectional injection into similar plasmas produces high toroidal rotation velocities (up to $\approx 10^6$ m/sec), lower central temperatures and densities, and ≈ 1 MA of net driven current for $P_B = 11$ MW which will be reported separately.

The surface voltage $V_{\text{sur}} \equiv [d\Psi/dt]_{\Phi}$, where Ψ and Φ are the surface poloidal and toroidal flux functions, respectively, is negative for these plasmas during beam heating, even with balanced injection for sufficiently large β_P , as shown in Fig. 2. V_{sur} is calculated with a filament current model¹⁶ to fit the magnetic measurements of the external poloidal field and flux, and is checked against six voltage loops distributed poloidally about the plasma. The fitting procedure is not completely compensated for vacuum-vessel eddy currents induced by rapid transient plasma motion during beam turn on and turn off. These perturbations decay on a time scale of ≈ 10 ms. The rapid decrease of V_{sur} in Fig. 1 from its prebeam value is partially explained by the measured fast changes in flux-surface shape, β_P (which changes the inductance), and T_e (which changes the resistivity). These discharges do not have sawtooth relaxations during beam heating, and show no evidence of disruptive MHD activity, which has previously¹⁷ been found to transiently force $V_{\text{sur}} < 0$. Thus, in the latter portion of the heating pulse, when the shape and I_p are constant, the continued expulsion of poloidal flux ($V_{\text{sur}} < 0$) is an indication of non-Ohmically driven currents.

To quantitatively understand the driven currents in these plasmas, the poloidal flux diffusion has been modeled by the time-dependent $1\frac{1}{2}$ -dimensional transport analysis code TRANSP.¹⁸ The code calculates the time evolution of V_{sur} for various assumptions of plasma

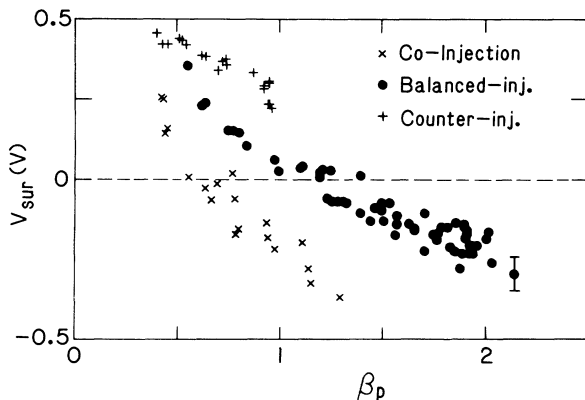


FIG. 2. Experimental variation of V_{sur} with β_P for cotangential neutral-beam injection, counter-tangential injection, and near-balanced cotangential and counter-tangential injection. The typical error bar is estimated from the sensitivity of the V_{sur} calculation to the location and number of filaments used to fit the magnetic measurements.

transport and driven currents, using measured time-dependent plasma parameters. The T_e and n_e profiles are measured at two times in each discharge by a 76-point Thomson scattering system.¹⁹ The T_e profile is also measured by first-harmonic electron-cyclotron-emission radiometry,²⁰ and the n_e profile by an array of vertical infrared interferometers.²¹ Central and near-central values of T_i and v_ϕ are measured spectroscopically, with Doppler broadening of FeXXV and FeXXIV lines. Z_{eff} is determined by tangential and radial measurements of visible bremsstrahlung emission and radial x-ray spectroscopy. Z_{eff} is assumed to be uniform for most of the calculations, in agreement with measurements made in other conditions. The shape and position of the outermost flux surface are deduced from the filament-current-model fit to the magnetic measurements. The measured profiles of n_e and T_e are mapped onto the calculated internal flux surface structure by a shift of the respective isocontours to the flux surfaces with the same horizontal minor diameter. This shift is typically < 3 cm, indicating good agreement between the calculated and experimental flux surfaces.

Neutral-beam deposition, orbiting, and thermalization are simulated by a Monte Carlo technique,²² calculating the fast-ion density, energy, and electrical current. Deposition by multistep ionization²³ can be calculated, but is not significant for this beam energy. The T_i profile was not measured for these plasmas, but is calculated from the ion energy-balance equation, with the assumption of $\chi_i = 2\chi_e$, classical electron-ion temperature equilibration, and a $\frac{3}{2}\Gamma T$ convective heat flow, in agreement with the analysis of T_i profile measurements on similar discharges.²⁴ The cross-field particle flow Γ is

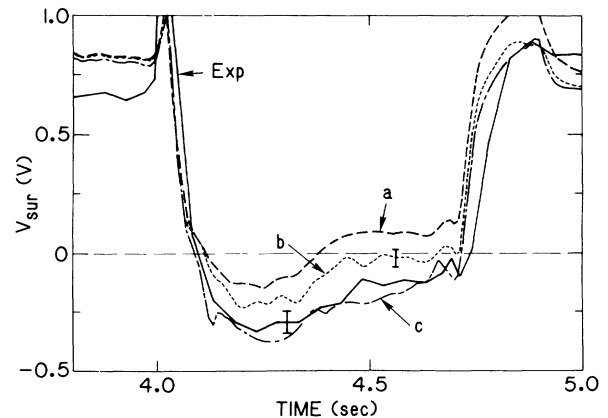


FIG. 3. The time variation of V_{sur} from experimental magnetic measurements (Exp) and calculated for various models: (a) Ohmic current, (b) beam-driven and Ohmic currents, and (c) bootstrap, beam-driven, and Ohmic currents for the plasma of Fig. 1. The typical error bar for the calculated V_{sur} is estimated from the sensitivity to τ_p , Z_{eff} profile, plasma shape, and other measured plasma parameters.

calculated from the continuity equation, the measured density and Z_{eff} , and the calculated beam and neutral-particle source rates. The global ion-particle confinement time τ_p is assumed to be 0.15 sec, consistent with limiter D_a measurements for similar plasmas. This analysis has been restricted to plasmas with nearly balanced momentum injection, avoiding the complications²⁵ introduced by the large rotation velocities obtained with unbalanced injection. Analysis has been completed for plasmas with up to 0.7 sec of neutral-beam heating. These simulations are in good agreement with the measured central impurity temperatures, the measured neutron flux, and magnetic measurements of stored energy, and indicate that $\approx 40\%$ of the total stored energy is due to unthermalized beam ions.

The electron shielding of the beam-ion current is calculated with inclusion of trapped-particle effects²⁶ and is small ($\approx 12\%$), as a result of the strength of electron trapping and the relatively large Z_{eff} . Thus uncertainties in Z_{eff} do not significantly affect the calculated net beam-driven current. The neoclassical bootstrap-current calculation^{26,27} includes the effects of impurity ions and finite aspect ratio, but does not include unthermalized beam ions. The calculated resistivity includes neoclassical trapped-particle corrections.²⁶

The measured V_{sur} for some of the low-density pre-beam target plasmas is slightly lower than the value calculated from the other measurements, but not as low as predicted with Spitzer resistivity²⁶ (without trapped-particle corrections). In these cases the target-current profile is also slightly broader than calculated, as indicated from magnetic measurements of Λ . Both effects appear to be due to high-energy nonthermal electrons, which are detected by the electron-cyclotron-emission diagnostics only in the prebeam phase. Long after the end of beam heating, when there is no indication of non-thermal electrons even though the density has decreased to close to the initial levels, the calculated V_{sur} and Λ approximately agree with the measured values. Calculations with phenomenologically increased conductivity to

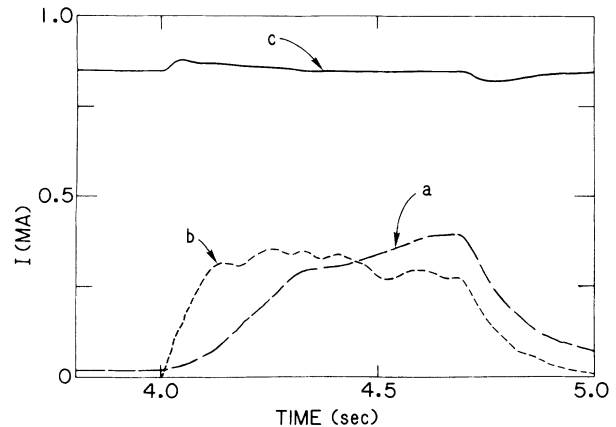


FIG. 4. Time dependence of (curve *a*) calculated bootstrap current, (curve *b*) calculated beam-driven current, and (curve *c*) measured total current for the plasma of Fig. 1.

match the prebeam V_{sur} , or an initially parabolic Z_{eff} profile to match V_{sur} and Λ , do not show significant differences from the results presented during the beam-heating pulse.

As shown in Fig. 3, during the beam-heating pulse the measured V_{sur} is well matched when the model includes both the neoclassical bootstrap current and the beam-driven current, but does not agree in the absence of the bootstrap current. Even though the injected beam power is nearly balanced, there is a substantial calculated beam-driven current (Fig. 4) due to the orientation of the counterinjected beams being closer to perpendicular to the magnetic field than that of the coinjected beams, and due to finite-width drift-orbit effects. The sum of the calculated non-Ohmic currents does not exceed I_p ; rather, the negative V_{sur} is due to the broadening of the current profile by the bootstrap current while the total current remains constant. The toroidal voltage remains positive on axis. The calculations also indicate that during the 0.7-sec heating pulse, V_{sur} is only sensitive to driven current in the outer 0.3 m of the plasma, because

TABLE I. Summary of time-dependent analyses after 0.5 sec of neutral-beam heating, showing the neutral-beam-heating power, fraction of cotangential power, plasma current, calculated bootstrap and beam-driven currents, and comparing the experimental voltage (V_{expt}) with the voltage predicted from Ohmic current alone (V_{Oh}), Ohmic and beam-driven current (V_{beam}), or Ohmic, beam, and bootstrap currents (V_{boot}).

| P_B (MW) | P_{co}/P_B | $\beta_{P\perp}$ | I_p (MA) | I_{boot} (MA) | I_{beam} (MA) | V_{Oh} (V) | V_{beam} (V) | V_{boot} (V) | V_{expt} (V) |
|---------------|---------------------|------------------|---------------|---------------------------|---------------------------|------------------------|--------------------------|--------------------------|--------------------------|
| 10.0 | 0.48 | 1.3 | 0.90 | 0.22 | 0.18 | 0.29 | 0.20 | -0.02 | 0.02 |
| 9.8 | 0.49 | 1.7 | 0.80 | 0.30 | 0.22 | 0.09 | 0.02 | -0.15 | -0.13 |
| 11.5 | 0.50 | 1.7 | 0.90 | 0.44 | 0.18 | 0.18 | 0.10 | -0.12 | -0.15 |
| 12.5 | 0.56 | 2.0 | 0.90 | 0.52 | 0.30 | 0.16 | 0.08 | -0.13 | -0.17 |
| 10.6 | 0.57 | 1.9 | 0.85 | 0.34 | 0.31 | 0.10 | -0.01 | -0.20 | -0.15 |
| 10.6 | 0.57 | 1.7 | 0.85 | 0.31 | 0.33 | 0.13 | 0.04 | -0.18 | -0.14 |
| 11.5 | 0.61 | 1.8 | 0.90 | 0.50 | 0.34 | 0.01 | 0.00 | -0.20 | -0.18 |

of the large electrical conductivity. For all plasmas analyzed in detail, Table I, it is necessary to include the bootstrap current in order to match the experimental V_{sur} .

No explanations of these observations not involving the bootstrap current have been found. In particular, variation of the value of Z_{eff} or its profile does not significantly increase the amount of beam-driven current, because of the lack of significant shielding current. To replace the calculated broad-profile bootstrap current, whose evolution matches the observed V_{sur} , by beam-driven current would require that $\approx 70\%$ of the calculated beam-driven current flow in the outer 0.3 m, where $n_e \approx 10^{19} \text{ m}^{-3}$. Since the beam-driven current is dominated by fast ions that have not slowed or pitch-angle scattered significantly, such a spatial rearrangement of the beam-driven current by fast-ion transport is incompatible with the observed plasma heating and $D(d,n)^3\text{He}$ neutron emission. V_{sur} can be roughly matched, without the bootstrap current, by the assumption that the atomic cross sections used in the calculation of beam deposition (primarily ionization and charge exchange with impurities) are too small in the 100-keV region by a factor of 3 to 5, well outside the accepted range of uncertainty.²⁸

In summary, substantial non-Ohmic currents are found in high- β_P neutral-beam-heated TFTR plasmas. Modeling of the plasma V_{sur} requires inclusion of the neoclassical bootstrap current.

We are grateful for the support of the TFTR group and for discussions with J. D. Callen, H. P. Furth, G. Hammett, K. McGuire, D. M. Meade, P. H. Rutherford, and J. D. Strachan. This work was supported by U.S. Department of Energy Contract No. DE-AC02-76-CHO-3073.

¹N. J. Fisch, *Rev. Mod. Phys.* **59**, 175 (1987).

²T. Ohkawa, *Nucl. Fusion* **10**, 185 (1970).

³A. A. Galeev, *Zh. Eksp. Teor. Fiz.* **59**, 1378 (1970) [*Sov. Phys. JETP* **32**, 752 (1971)].

⁴R. J. Bickerton, J. W. Connor, and J. B. Taylor, *Nature (London) Phys. Sci.* **229**, 110 (1971).

⁵D. F. H. Start *et al.*, *Phys. Rev. Lett.* **40**, 1497 (1978).

⁶W. H. M. Clark *et al.*, *Phys. Rev. Lett.* **45**, 1101 (1980).

⁷S. Besshou *et al.*, *Plasma Phys.* **26**, 565 (1984).

⁸A. H. Boozer, *Phys. Fluids* **29**, 4123 (1986).

⁹M. S. Berezhtsky *et al.*, in *Plasma Physics and Controlled Thermonuclear Fusion Research* (International Atomic Energy Agency, Vienna, 1971), Vol. 3, p. 49.

¹⁰R. A. E. Bolton *et al.*, Ref. 9, p. 79.

¹¹J. D. Treffert, J. L. Shohet, and H. L. Berk, *Phys. Rev. Lett.* **53**, 2409 (1984).

¹²J. T. Hogan, *Nucl. Fusion* **21**, 365 (1981).

¹³M. C. Zarnstorff and S. C. Prager, *Phys. Fluids* **29**, 308 (1986).

¹⁴K. C. Shaing, S. P. Hirshman, and J. D. Callen, *Phys. Fluids* **29**, 521 (1986).

¹⁵J. D. Strachan *et al.*, *Phys. Rev. Lett.* **58**, 1004 (1987).

¹⁶D. W. Swain and G. H. Neilson, *Nucl. Fusion* **22**, 1015 (1982).

¹⁷I. H. Hutchinson, *Phys. Rev. Lett.* **37**, 338 (1976).

¹⁸R. J. Hawryluk, in *Physics of Plasmas Close to Thermonuclear Conditions*, edited by B. Coppi *et al.* (Commission of the European Communities, Brussels, 1980), Vol. 1, p. 19.

¹⁹D. Johnson *et al.*, *Rev. Sci. Instrum.* **57**, 1856 (1986).

²⁰G. Taylor *et al.*, *Rev. Sci. Instrum.* **55**, 1739 (1984).

²¹D. K. Mansfield *et al.*, *Appl. Opt.* **26**, 4469 (1987).

²²R. J. Goldston *et al.*, *J. Comput. Phys.* **43**, 61 (1981).

²³C. D. Boley, R. K. Janev, and D. E. Post, *Phys. Rev. Lett.* **52**, 534 (1984).

²⁴R. J. Fonck *et al.*, *Bull. Am. Phys. Soc.* **32**, 1846 (1987).

²⁵R. J. Goldston, in *Basic Physical Processes of Toroidal Fusion Plasmas*, edited by G. P. Lampis *et al.* (Commission of the European Communities, Brussels, 1986), Vol. 1, p. 165.

²⁶S. P. Hirshman and D. J. Sigmar, *Nucl. Fusion* **21**, 1079 (1981).

²⁷S. P. Hirshman, *Phys. Fluids* **21**, 1295 (1978).

²⁸R. A. Phaneuf *et al.*, Oak Ridge National Laboratory Technical Report No. ORNL-6090, 1987 (to be published).